A Photometric Study of the Near-Contact Binary XZ Persei

Edward J. Michaels
Stephen F. Austin State University, Department of Physics, Engineering, and Astronomy, P.O. Box 13044, Nacogdoches, TX 75962; emichaels@sfasu.edu

Received February 6, 2017; revised March 1, 2017; accepted March 1, 2017

Abstract Presented are two sets of multi-band CCD photometry of the Algol-type binary XZ Persei. Photometric solutions were derived using the Wilson-Devinney program for each dataset. The solution results indicate XZ Per is a semi-detached, near-contact binary whose less-massive secondary star fills its Roche lobe. Asymmetries in the light curves were modeled by including a hot spot on the primary star. This spot is likely caused by impact heating from mass transfer. The orbital period was analyzed using 473 light minima spanning 90 years. Several alternating period changes were found superimposed on a long term secular period decrease. With continued mass and angular momentum loss, the separation between the stars will likely decrease until the primary fills its Roche lobe forming a contact binary.

1. Introduction

The *General Catalogue of Variable Stars* (GCVS; Samus *et al.* 2017) identifies XZ Persei (TYC 3328-3186-1, GSC 3328-3186) as a semi-detached Algol eclipsing system with an orbital period of 1.15163412 days and a spectral type of G1. Photometric orbital elements were first determined by Lavrov (1971). Geometric and physical parameters for this system were computed by Brancewicz and Dworak (1980) using an iterative method which indicated a semi-detached configuration. XZ Per is also included in a catalogue of 411 Algol-type binary stars (Budding *et al.* 2004). This catalogue gives an orbital inclination of 88°, a mass ratio of 0.69, a distance of 250 pc, and spectral types for the primary and secondary stars of G1+[K1IV]. In a spectroscopic survey of late F-K eclipsing binaries, Popper (1996) found the primary star's spectral type to be F2-5. Many primary minima timings have been published going back to 1927. Several period studies have been completed on this system (Whitney 1959; Szafraniec 1960; Wood and Forbes 1963; Kreiner 1971; Mallama 1980; Qian 2001a). It has also been surveyed for a gaseous disk using time-resolved spectroscopy (Kaitchuck and Honeycutt 1982; Kaitchuck *et al.* 1985).

In this paper a photometric study of XZ Per is presented. The paper is organized into sections. The first complete set of multi-wavelength photometric observations for this star is presented in section 2. Orbital period changes are investigated in section 3, a light curve analysis is presented in section 4, results from the period study and light curve analysis are discussed in section 5, and conclusions are stated in section 6.

2. Observations

XZ Per was observed photometrically with the 0.31-m Ritchey-Chrétien telescope located at the Waffelow Creek Observatory (http://obs.ejmj.net/index.php). Images were acquired with a SBIG-STXL camera equipped with a KAF-6303E CCD (9μm pixels). Two complete data sets were collected. Images that comprise Data Set 1 (DS1) were taken in the Sloan g', r', and i' passbands on fifteen nights in January and February 2016. Data Set 2 (DS2) images were acquired in the Johnson B and V passbands on eight nights in September and October 2016. A total of 7,226 images were acquired, 4,648 in the Sloan passbands and 2,578 in the Johnson passbands. All the images were calibrated with bias, dark, and flat field frames taken before each night's observing run. MIRA software was used for calibration and ensemble differential aperture photometry of the light images (Mirametrics 2015). The instrumental magnitudes of XZ Per were converted to standard magnitudes using comparison star magnitudes taken from the AAVSO Photometric All-Sky Survey (APASS; Henden *et al.* 2014). The comparison and check stars used in this study are shown in Table 1. The finder chart in Figure 1 shows a nearby field star 8.1" to the ENE of XZ Per. The light contribution from this star was easily removed by proper sizing of the rings when performing the aperture photometry. After converting the Heliocentric Julian Day (HJD) of each observation to orbital phase the folded light curves were plotted (see Figure 2). All light curves in this paper are plotted from phase –0.6 to 0.6, with negative phase defined as $\varphi - 1$. The check star's V passband observations are shown in the bottom panel of Figure 2 with the standard deviations shown in Table 1. The check star magnitudes were inspected each night and no significant variability was found. The observations have been archived and are accessible from the AAVSO International Database (Kafka 2015).

3. Analysis

3.1. Period study and ephemerides

The most recent study of orbital period changes for XZ Per was done by Qian (2001a). Since that study, many additional minimum timings have become available and were used in the present analysis. From the literature, 488 minima were found spanning the years 1927–2016. From the observations in this study, an additional seven new primary minima were obtained (Table 2). Using the linear ephemeris of Mallama (1980),

$$\text{HJD Min I} = 2443507.47742 + 1.15163412\ E, \qquad (1)$$

the *(O–C)* values were computed. All the minima timings and *(O–C)* values are listed in Tables 2 and 3. The ephemeris diagram is shown in Figure 3. From the full set of minima, fifteen timings identified in Table 3 showed significant deviations from the

Table 1. Variable (V), comparison (C), and check (K) stars in this study.

Star	*R.A. (2000) h*	*Dec. (2000) °*	*B*	*V*	*g′*	*r′*	*i′*	*(B–V)*
XZ Per (V)	4.15768	+46.56686						
GSC3328-1649 (C1)	4.17230	+46.48831	11.295 ± 0.076	10.570 ± 0.059	10.882 ± 0.052	10.372 ± 0.065	10.239 ± 0.043	0.725
GSC3328-1055 (C2)	4.16805	+46.60359	11.662 —	10.746 ± 0.012	11.167 ± 0.049	10.456 ± 0.012	10.116 ± 0.034	0.916
GSC3328-2924 (C3)	4.16396	+46.50468	11.410 —	10.911 ± 0.019	11.118 ± 0.037	10.795 ± 0.015	10.639 ± 0.039	0.499
GSC3328-2029 (C4)	4.15812	+46.62578	11.837 —	11.181 ± 0.025	11.447 ± 0.032	10.982 ± 0.010	10.761 ± 0.028	0.656
GSC3328-985 (C5)	4.17478	+46.52096	12.374 ± 0.008	11.386 ± 0.045	11.866 ± 0.010	10.957 ± 0.017	10.419 ± 0.000	0.998
GSC3328-1883 (C6)	4.16236	+46.67258	12.291 ± 0.008	11.725 ± 0.030	11.966 ± 0.035	11.574 ± 0.006	11.391 ± 0.033	0.566
GSC3328-1869 (C7)	4.14996	+46.46364	12.497 ± 0.038	11.810 ± 0.059	12.085 ± 0.034	11.601 ± 0.034	11.415 ± 0.059	0.687
GSC3328-2491 (C8)	4.13869	+46.45859	12.681 ± 0.049	12.064 ± 0.060	12.303 ± 0.033	11.921 ± 0.029	11.764 ± 0.067	0.617
GSC3328-2529 (C9)	4.16223	+46.66057	13.079 ± 0.006	12.260 ± 0.034	12.603 ± 0.029	11.982 ± 0.006	11.655 ± 0.020	0.819
GSC3328-1641 (K)	4.14319	+46.54925	13.418 —	11.829 ± 0.017	12.553 ± 0.025	11.244 ± 0.000	10.606 ± 0.020	1.589
Standard deviation of check star magnitudes			± 0.016	± 0.008	± 0.008	± 0.006	± 0.006	
Observed check star magnitudes (K)			13.421 ± 0.049	11.815 ± 0.023	12.532 ± 0.029	11.247 ± 0.023	10.607 ± 0.023	

APASS comparison and check star magnitudes and errors. The observed check star magnitudes are the averages over all nights for each passband.

Table 2. New times of minima for XZ Per.

Epoch HJD 2400000+	*Error*	*Type*	*Cycle*	*O–C*
57400.7189	0.00012	ccd	12064.0	–0.07256
57422.5998	0.00010	ccd	12083.0	–0.07264
57423.7515	0.00013	ccd	12084.0	–0.07258
57430.6614	0.00010	ccd	12090.0	–0.07251
57666.7458	0.00004	ccd	12295.0	–0.07309
57667.8977	0.00006	ccd	12296.0	–0.07283
57689.7785	0.00005	ccd	12315.0	–0.07314

trend and were therefore not used in the analysis.

Using the *(O–C)* residuals from Equation 1, a new linear ephemeris was computed by weighted least-squares solution. A weight of 1 was applied to visual and photographic timings, and 10 to PE and CCD observations. The new linear ephemeris is given by

$$\text{HJD Min I} = 2457689.78840(8) + 1.15163048(9)\,E, \quad (2)$$

and is shown overlaid on the O–C data in Figure 3 (dashed line). The general *(O–C)* trend indicates the orbital period appears to be slowly decreasing with embedded sudden alternating period jumps. This behavior was first noted by Qian (2001a), who found the period variation to consist of a secular period decrease with two superposed period jumps. Since that study, it appears several additional period jumps have occurred (see Figure 3). Assuming the *(O–C)* data trend has a parabolic variation that is not a part of a longer repeating cycle, a weighted least-squares

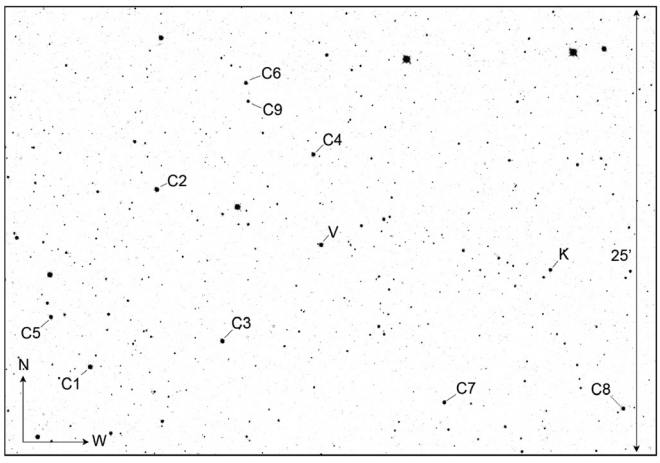

Figure 1. Finder chart for XZ Per (V), comparison (C1–C9), and check (K) stars.

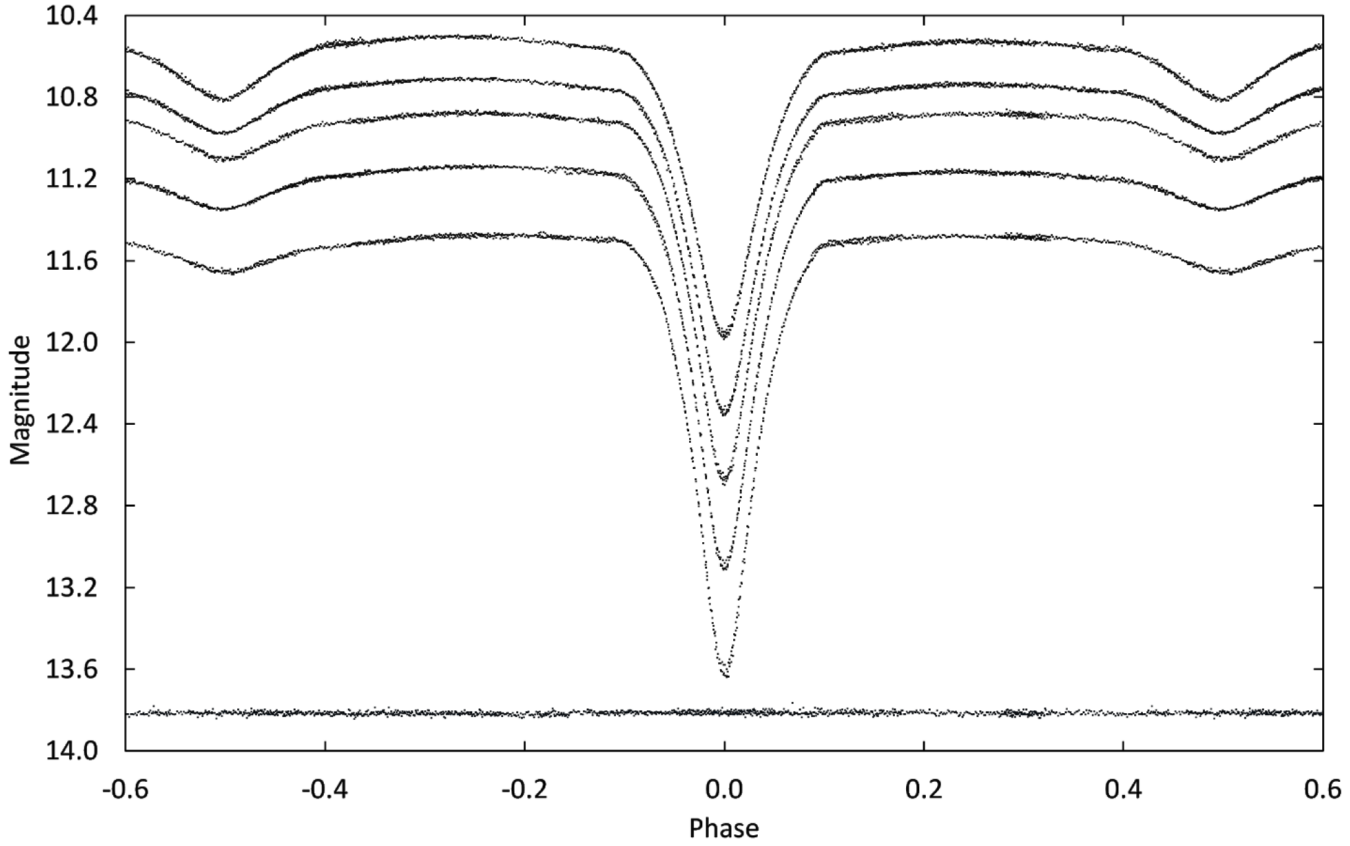

Figure 2. Folded light curves for each observed passband. The differential magnitudes of the variable were converted to standard magnitudes using the calibrated magnitudes of the comparison stars. From top to bottom the light curve passbands are Sloan i', Sloan r', Johnson V, Sloan g', and Johnson B. The bottom curve shows the standard Johnson V magnitudes of the check star (offset +2.0 magnitude). The standard deviations of the check star magnitudes are shown in Table 1. Error bars are not shown for clarity.

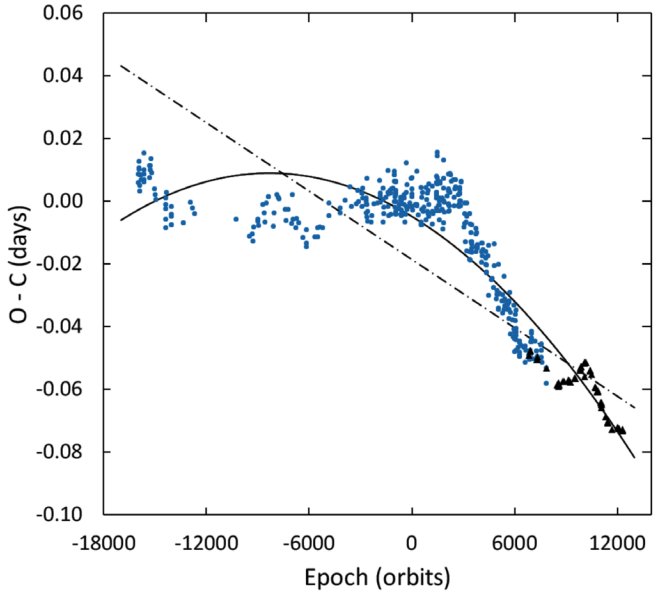

Figure 3. (*O–C)* residuals from the linear ephemeris of Equation 1. The dashed line is the new linear fit of Equation 2 and the solid line the quadratic fit of Equation 3. Circles refer to visual and photographic data and triangles the PE and CCD data.

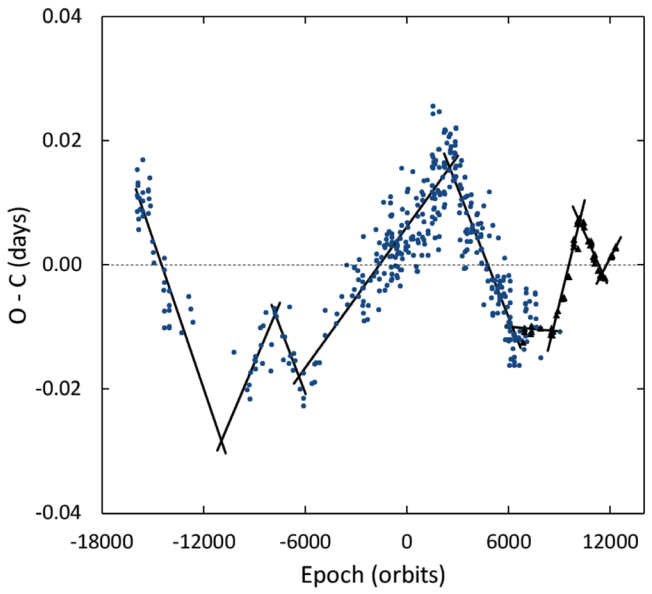

Figure 4. $(O–C)_Q$ residuals from the quadratic ephemeris fit. The line segments are several linear ephemerides that were fit to the residuals. Circles refer to visual and photographic data and triangles the PE and CCD data.

solution yields the following quadratic ephemeris:

$$\text{HJD Min I} = 2457689.7909(7) + 1.15162587(6)\,E - 3.48(12)\times10^{-10}E^2. \quad (3)$$

The quadratic fit to the *(O–C)* observations is shown in Figure 3 (solid line) and the $(O–C)_Q$ residuals from the quadratic ephemeris are presented in Figure 4.

The $(O–C)_Q$ residuals clearly show the decreasing period is not smooth but punctuated by several alternating period changes. It is assumed that between the period jumps the orbital period is undergoing a steady decrease. From inspection of Figure 4, there appear to be 8 period jumps. To better characterize the period jumps, the $(O–C)_Q$ residuals were divided into nine segments (see Figure 4). Using the method of least-squares, a linear function given by

$$(O–C)_Q = \Delta T + \Delta P E\,, \quad (4)$$

was found for each segment to obtain the best fit to the $(O–C)_Q$ values. The computed ΔT and ΔP values for each segment are listed in Table 4. For any cycle E the orbital period, P(E), can be computed by summing the ephemeris period (P_E = 1.15163412 days), the period jump for the segment in which the cycle is located (ΔT), and the contribution from the secular period decrease using dP/dt in units of days/day ($dP/dt = -3.48 \times 10^{-10}$ d d^{-1}). Using the following equation,

$$P(E) = P_E + \Delta P + \frac{dP}{dt} EP\,, \quad (5)$$

the differences between the actual period P(E) and the ephemeris period P_E for each segment were computed and the results plotted in Figure 5. It is possible some of the early jumps located between cycles –16,000 and –6,000 are not real. This cycle interval has fewer observations, the visual minima have a large amount of scatter, and a large data gap exists for the years 1938–1945. More precise CCD minima timings became available beginning about the year 1999 (cycle count 7,000). Between cycles 7,000 and 15,000 a few sudden period changes are well documented by these precision timings, leaving little doubt that period jumps are occurring in this system.

3.2. Temperature, spectral type

Popper (1996) obtained three high-resolution spectra of XZ Per and found a spectral type of F2-5. The spectral lines of only the primary star were seen. For light curve modeling an effective temperature for the primary was selected midway between the spectral types F2 and F5 with an error estimate taken from that range. Using Table 5 of Pecaut and Mamajek (2013) gives an effective temperature for the primary star of T_{eff} = 6680 ± 170K and a color index of $B–V$ = 0.40 ± 0.05. To measure the changing color of XZ Per over its entire phase range, the Johnson *V* and *B* passband observations were binned with a phase width of 0.005. Both phase and magnitude were averaged in each bin interval. Figure 6 shows the binned V magnitude light curve and in the bottom panel the *(B–V)* color index. The significant reddening of the light at primary eclipse indicates a large temperature difference between the primary and secondary stars. The observed color over the entire phase range may also be reddened due to interstellar dust. XZ Per is located 3° south of the galactic equator, therefore a significant amount of interstellar extinction is possible. Extinction will be discussed further in section 4.

3.3. Synthetic light curve modeling

Photometric models of XZ Per were obtained for each of the two sets of data, DS1 (g', r', and i' observations) and DS2 (*B* and *V* observations). The observations were binned in both phase and magnitude with a phase interval of 0.005. The average number of observations per bin was eight for DS1 and six for DS2. The binned magnitudes were converted to relative flux for modeling. Preliminary fits to each light curve were made using the BINARY MAKER 3.0 program (BM3; Bradstreet and Steelman 2002). The initial mass ratio for this modeling was taken from a catalogue of eclipsing binary parameters (Brancewicz and Dworak 1980); standard convective parameters were used for both stars and limb darkening coefficients were from Van Hamme's (1993) tabular values. The resulting BM3 synthetic light curves for each color fit the observations well and were consistent for each data set. The stellar parameters from the light curve fits were independently averaged for each model, DS1 and DS2. These values were used as the initial input parameters for computation of simultaneous three-color (DS1) and two-color (DS2) light curve solutions with the 2013 version of the Wilson-Devinney program (WD; Wilson and Devinney 1971; Van Hamme and Wilson 1998). There are two mass ratios published for this system, 0.69 (Brancewicz and Dworak 1980) and 0.50 (Malkov *et al.* 2006). A derived mass ratio from a WD solution would only have reasonable accuracy if the eclipses are total (Wilson 1978; Terrell and Wilson 2005). The eclipses of XZ Per are not total, and combined with the inconsistent published mass ratios, a q-search would be required. For fixed inputs, the effective temperature of the primary was set to T_1 = 6680 K (see section 3.2) and standard convective values for gravity darkening and albedo, $g_1 = g_2 = 0.32$ (Lucy 1968) and $A_1 = A_2 = 0.5$ (Ruciński 1969), respectively. The logarithmic limb darkening coefficients were interpolated from tabulated values using the method of Van Hamme (1993). The Kurucz (1993) stellar atmosphere model was applied and detailed reflection was utilized in modeling. The adjustable parameters include the inclination (i), mass ratio ($q = M_2 / M_1$), potential (Ω), temperature of the secondary star (T_2), the normalized flux for each wavelength (L), and third light (ℓ).

Mode 2 (detached configuration) was used initially but every solution attempt converged quickly to a semi-detached configuration. This indicates the secondary star fills its Roche lobe. Mode 5 (semi-detached configuration) was therefore used on subsequent iterations and the final solutions. Using the DS1 light curves, a series of solutions were made using fixed mass ratios from 0.30 to 1.00 with a step of 0.05. This q-search had minimum residual value at about q = 0.64 (see Figure 7) and was used as the initial mass ratio for the final solution attempts for each data set. With the mass ratio as a free parameter, the resulting best-fit final solution parameters are shown in columns

Table 3. Available times of minima and O–C residuals from Equation 1.

Epoch HJD 2400000+	*Type*	*Cycle*	*O–C*	*Reference*
25150.438	vis	–15940.0	0.00847	BAV Lichten. DB
25151.587	vis	–15939.0	0.00584	BAV Lichten. DB
25157.352	vis	–15934.0	0.01267	BAV Lichten. DB
25187.292	vis	–15908.0	0.01018	BAV Lichten. DB
25188.444	vis	–15907.0	0.01055	BAV Lichten. DB
25216.081	vis	–15883.0	0.00833	BAV Lichten. DB
25234.502	vis	–15867.0	0.00318	BAV Lichten. DB
25249.475	vis	–15854.0	0.00494	BAV Lichten. DB
25301.302	vis	–15809.0	0.00840	BAV Lichten. DB
25324.333	vis	–15789.0	0.00672	BAV Lichten. DB
25506.293	vis	–15631.0	0.00853	BAV Lichten. DB
25514.352	vis	–15624.0	0.00609	BAV Lichten. DB
25520.114	vis	–15619.0	0.00992	BAV Lichten. DB
25529.324	vis	–15611.0	0.00685	BAV Lichten. DB
25530.484	vis	–15610.0	0.01521	BAV Lichten. DB
25886.335	vis	–15301.0	0.01127	BAV Lichten. DB
25893.241	vis	–15295.0	0.00747	BAV Lichten. DB
25917.429	vis	–15274.0	0.01115	BAV Lichten. DB
25945.067	vis	–15250.0	0.00993	BAV Lichten. DB
26000.349	vis	–15202.0	0.01349	BAV Lichten. DB
26030.287	vis	–15176.0	0.00901	BAV Lichten. DB
26208.785	vis	–15021.0	0.00372	BAV Lichten. DB
26257.152	vis	–14979.0	0.00208	BAV Lichten. DB
26305.519	vis	–14937.0	0.00045	BAV Lichten. DB
26957.341	vis	–14371.0	–0.00246	BAV Lichten. DB
26979.216	vis	–14352.0	–0.00851	BAV Lichten. DB
26980.375	vis	–14351.0	–0.00114	BAV Lichten. DB
26980.377	vis	–14351.0	0.00086	BAV Lichten. DB
26981.522	vis	–14350.0	–0.00578	BAV Lichten. DB
27002.260	vis	–14332.0	0.00281	BAV Lichten. DB
27337.375	vis	–14041.0	–0.00772	BAV Lichten. DB
27343.136	vis	–14036.0	–0.00489	BAV Lichten. DB
27344.285	vis	–14035.0	–0.00753	BAV Lichten. DB
27345.440	vis	–14034.0	–0.00416	BAV Lichten. DB
27346.594	vis	–14033.0	–0.00179	BAV Lichten. DB
28151.581	vis	–13334.0	–0.00704	BAV Lichten. DB
28151.581	vis	–13334.0	–0.00704	BAV Lichten. DB
28635.274	vis	–12914.0	–0.00037	BAV Lichten. DB
28783.833	vis	–12785.0	–0.00218	BAV Lichten. DB
28932.392	vis	–12656.0	–0.00398	BAV Lichten. DB
31712.435	vis	–10242.0	–0.00574	BAV Lichten. DB
32623.372	vis	–9451.0	–0.01133	BAV Lichten. DB
32770.782	vis	–9323.0	–0.01050	BAV Lichten. DB
32820.300	vis	–9280.0	–0.01277	BAV Lichten. DB
32868.673	vis	–9238.0	–0.00840	BAV Lichten. DB
33155.432	vis	–8989.0	–0.00630	BAV Lichten. DB
33183.071	vis	–8965.0	–0.00651	BAV Lichten. DB
33185.375	vis	–8963.0	–0.00578	BAV Lichten. DB
33207.254	vis	–8944.0	–0.00783	BAV Lichten. DB
33505.534	vis	–8685.0	–0.00107	BAV Lichten. DB
33581.539	vis	–8619.0	–0.00392	BAV Lichten. DB
33657.544	vis	–8553.0	–0.00677	BAV Lichten. DB
33717.435	P	–8501.0	–0.00075	BAV Lichten. DB
33900.547	vis	–8342.0	0.00143	BAV Lichten. DB
33900.547	vis	–8342.0	0.00143	BAV Lichten. DB
34226.450	vis	–8059.0	–0.00803	BAV Lichten. DB
34271.368	vis	–8020.0	–0.00376	BAV Lichten. DB
34284.334*	vis	–8008.5	–0.28155	BAV Lichten. DB
34453.332	vis	–7862.0	0.00205	BAV Lichten. DB
34529.339	vis	–7796.0	0.00120	BAV Lichten. DB
34606.498	vis	–7729.0	0.00071	BAV Lichten. DB
35008.415	vis	–7380.0	–0.00259	BAV Lichten. DB
35008.415	vis	–7380.0	–0.00259	BAV Lichten. DB
35062.538	P	–7333.0	–0.00640	Whitney 1959
35190.373	P	–7222.0	–0.00279	BAV Lichten. DB
35450.638	P	–6996.0	–0.00710	Whitney 1959
35510.532	P	–6944.0	0.00193	Whitney 1959
35539.315	P	–6919.0	–0.00592	BAV Lichten. DB
35745.455	vis	–6740.0	–0.00843	BAV Lichten. DB
35782.310	vis	–6708.0	–0.00572	BAV Lichten. DB
35904.382	vis	–6602.0	–0.00694	BAV Lichten. DB
36194.589	P	–6350.0	–0.01174	Whitney 1959
36452.552	vis	–6126.0	–0.01458	BAV Lichten. DB
36452.553	vis	–6126.0	–0.01338	BAV Lichten. DB
36452.558	vis	–6126.0	–0.00928	BAV Lichten. DB
37020.311	vis	–5633.0	–0.01140	BAV Lichten. DB
37196.511	vis	–5480.0	–0.01142	BAV Lichten. DB
37196.514	vis	–5480.0	–0.00842	BAV Lichten. DB
37316.284	vis	–5376.0	–0.00837	BAV Lichten. DB
37545.459	vis	–5177.0	–0.00856	BAV Lichten. DB
37932.412	vis	–4841.0	–0.00463	BAV Lichten. DB
37932.416	vis	–4841.0	–0.00063	BAV Lichten. DB
38684.430	P	–4188.0	–0.00371	Todoran 1967
38714.374	P	–4162.0	–0.00219	Todoran 1967
39033.379	vis	–3885.0	0.00016	BAV Lichten. DB
39390.390	P	–3575.0	0.00458	Todoran 1967
39445.662	vis	–3527.0	–0.00186	Robinson 1967
39772.727	vis	–3243.0	–0.00095	Baldwin 1974
39886.743	vis	–3144.0	0.00327	Baldwin 1974
39893.653	vis	–3138.0	0.00347	Baldwin 1974
39916.682	vis	–3118.0	–0.00021	Baldwin 1974
40151.618	vis	–2914.0	0.00243	BAV Lichten. DB
40151.618	P	–2914.0	0.00243	Baldwin 1974
40188.466	vis	–2882.0	–0.00187	Flin 1969
40203.440	vis	–2869.0	0.00089	Flin 1969
40232.234	vis	–2844.0	0.00404	Flin 1969
40471.766	vis	–2636.0	–0.00386	Baldwin 1974
40477.527	vis	–2631.0	–0.00103	BAV Lichten. DB
40477.528	vis	–2631.0	–0.00003	BAV Lichten. DB
40477.529	vis	–2631.0	0.00097	BAV Lichten. DB
40499.404	vis	–2612.0	–0.00508	BAV Lichten. DB
40499.408	vis	–2612.0	–0.00108	BAV Lichten. DB
40500.568	vis	–2611.0	0.00729	BAV Lichten. DB
40539.713	vis	–2577.0	–0.00327	Baldwin 1974
40554.681	vis	–2564.0	–0.00652	Baldwin 1974
40796.524	vis	–2354.0	–0.00668	BAV Lichten. DB
40856.411	vis	–2302.0	–0.00466	Baldwin 1975
40969.275	vis	–2204.0	–0.00080	Baldwin 1976a
41221.483	vis	–1985.0	–0.00067	BAV Lichten. DB
41357.383	vis	–1867.0	0.00650	Klimek 1972
41395.380	vis	–1834.0	–0.00042	Klimek 1973
41395.382	vis	–1834.0	0.00158	BBSAG No. 2
41395.383	vis	–1834.0	0.00258	Baldwin 1976a
41410.353	vis	–1821.0	0.00133	BBSAG No. 3
41570.422	vis	–1682.0	–0.00681	BBSAG No. 5
41585.404	vis	–1669.0	0.00395	BBSAG No. 5
41593.462	vis	–1662.0	0.00051	BBSAG No. 6
41623.400	vis	–1636.0	–0.00398	BBSAG No. 6
41623.402	vis	–1636.0	–0.00198	Baldwin 1976a
41759.298	vis	–1518.0	0.00119	BBSAG No. 8
41905.564	vis	–1391.0	0.00966	BBSAG No. 11
41913.614	vis	–1384.0	–0.00178	BBSAG No. 11
41927.438	vis	–1372.0	0.00261	BBSAG No. 11
41982.716	vis	–1324.0	0.00217	Baldwin 1976b
41989.619	vis	–1318.0	–0.00463	Baldwin 1976b
42071.393	vis	–1247.0	0.00335	BBSAG No. 13
42109.396	vis	–1214.0	0.00242	BBSAG No. 14
42132.422	vis	–1194.0	–0.00426	BBSAG No. 14
42139.340	vis	–1188.0	0.00393	BBSAG No. 15
42262.565	vis	–1081.0	0.00408	BBSAG No. 17
42337.417	vis	–1016.0	–0.00013	BBSAG No. 18
42367.366	vis	–990.0	0.00638	BAV Lichten. DB
42367.368	vis	–990.0	0.00838	BAV Lichten. DB
42367.368	vis	–990.0	0.00838	BAV Lichten. DB

table continued on following pages

Table 3. Available times of minima and O–C residuals from Equation 1, cont.

Epoch HJD 2400000+	Type	Cycle	O–C	Reference	Epoch HJD 2400000+	Type	Cycle	O–C	Reference
42367.369	vis	–990.0	0.00938	BAV Lichten. DB	44638.378	vis	982.0	–0.00411	BAV Lichten. DB
42391.542	vis	–969.0	–0.00194	Baldwin 1977	44646.449	vis	989.0	0.00546	BBSAG No. 53
42405.365	vis	–957.0	0.00145	BBSAG No. 19	44647.594	vis	990.0	–0.00118	Baldwin and Samolyk 1993
42428.392	vis	–937.0	–0.00423	BBSAG No. 20	44683.291	vis	1021.0	–0.00484	BBSAG No. 53
42429.554	vis	–936.0	0.00614	BAV Lichten. DB	44881.358*	vis	1193.0	–0.01891	BAV Lichten. DB
42435.302	vis	–931.0	–0.00403	BBSAG No. 20	44883.685	vis	1195.0	0.00483	BBSAG No. 57
42435.308	vis	–931.0	0.00197	BBSAG No. 20	44884.839*	vis	1196.0	0.00719	Baldwin and Samolyk 1993
42450.274	vis	–918.0	–0.00328	BBSAG No. 21	44898.648	vis	1208.0	–0.00342	Baldwin and Samolyk 1993
42450.277	vis	–918.0	–0.00028	BBSAG No. 21	44911.312	vis	1219.0	–0.00739	BBSAG No. 57
42450.280	vis	–918.0	0.00272	BBSAG No. 21	44934.348	vis	1239.0	–0.00407	BBSAG No. 57
42458.342	vis	–911.0	0.00328	BBSAG No. 21	45201.528	vis	1471.0	–0.00319	BAV Lichten. DB
42458.345	vis	–911.0	0.00628	BBSAG No. 21	45201.529	vis	1471.0	–0.00219	BAV Lichten. DB
42688.663	vis	–711.0	–0.00254	BAV Lichten. DB	45201.532	vis	1471.0	0.00081	BAV Lichten. DB
42689.816	vis	–710.0	–0.00117	BAV Lichten. DB	45201.532	vis	1471.0	0.00081	BAV Lichten. DB
42754.309	vis	–654.0	0.00031	BBSAG No. 25	45201.533	vis	1471.0	0.00181	BAV Lichten. DB
42777.337	vis	–634.0	–0.00437	BBSAG No. 25	45201.533	vis	1471.0	0.00181	BAV Lichten. DB
42785.404	vis	–627.0	0.00119	BBSAG No. 26	45201.534	vis	1471.0	0.00281	BAV Lichten. DB
42809.587	vis	–606.0	–0.00012	Baldwin and Samolyk 1993	45201.534	vis	1471.0	0.00281	BAV Lichten. DB
42830.317	vis	–588.0	0.00046	BBSAG No. 26	45201.534	vis	1471.0	0.00281	BAV Lichten. DB
42832.615	vis	–586.0	–0.00481	Baldwin and Samolyk 1993	45201.537	vis	1471.0	0.00581	BAV Lichten. DB
42832.620	vis	–586.0	0.00019	Baldwin and Samolyk 1993	45201.537	vis	1471.0	0.00581	BAV Lichten. DB
42838.375	vis	–581.0	–0.00298	BBSAG No. 26	45201.539	vis	1471.0	0.00781	BAV Lichten. DB
42838.377	vis	–581.0	–0.00098	BBSAG No. 26	45231.481	vis	1497.0	0.00732	BBSAG No. 62
42985.786	vis	–453.0	–0.00114	Baldwin and Samolyk 1993	45247.602	vis	1511.0	0.00544	BBSAG No. 63
43014.580	vis	–428.0	0.00200	BBSAG No. 29	45247.612	vis	1511.0	0.01544	BBSAG No. 63
43023.787	vis	–420.0	–0.00407	Baldwin and Samolyk 1993	45253.369	vis	1516.0	0.01427	BBSAG No. 63
43023.792	vis	–420.0	0.00093	BAV Lichten. DB	45313.246	vis	1568.0	0.00630	BBSAG No. 64
43037.604	vis	–408.0	–0.00668	BBSAG No. 30	45314.390	vis	1569.0	–0.00133	BBSAG No. 64
43098.643	vis	–355.0	–0.00429	Baldwin and Samolyk 1993	45352.394	vis	1602.0	–0.00126	BBSAG No. 64
43128.588	vis	–329.0	–0.00177	Baldwin and Samolyk 1993	45359.306	vis	1608.0	0.00094	BBSAG No. 64
43134.360	vis	–324.0	0.01205	BAV Lichten. DB	45368.512	vis	1616.0	–0.00614	BBSAG No. 65
43136.654	vis	–322.0	0.00279	Baldwin and Samolyk 1993	45390.396	vis	1635.0	–0.00319	BBSAG No. 65
43188.472	vis	–277.0	–0.00275	BBSAG No. 32	45397.309	vis	1641.0	0.00001	BBSAG No. 65
43188.480	vis	–277.0	0.00525	BBSAG No. 32	45405.376	vis	1648.0	0.00557	BBSAG No. 66
43393.465	vis	–99.0	–0.00062	BBSAG No. 35	45435.319	vis	1674.0	0.00608	BBSAG No. 66
43395.767	vis	–97.0	–0.00189	Baldwin and Samolyk 1993	45558.535	vis	1781.0	–0.00277	BAV Lichten. DB
43409.587	vis	–85.0	–0.00150	BBSAG No. 35	45566.600	vis	1788.0	0.00079	BBSAG No. 68
43493.665	vis	–12.0	0.00721	Baldwin and Samolyk 1993	45611.504	vis	1827.0	–0.00894	BBSAG No. 69
43506.328	vis	–1.0	0.00223	BBSAG No. 36	45640.311	vis	1852.0	0.00721	BBSAG No. 69
43514.391	vis	6.0	0.00380	BBSAG No. 36	45649.510	vis	1860.0	–0.00686	BBSAG No. 69
43538.579	vis	27.0	0.00748	Baldwin and Samolyk 1993	45671.398	vis	1879.0	0.00009	BAV Lichten. DB
43544.328	vis	32.0	–0.00169	BBSAG No. 36	45671.402	vis	1879.0	0.00409	BAV Lichten. DB
43544.331	vis	32.0	0.00131	BBSAG No. 36	45671.405	vis	1879.0	0.00709	BAV Lichten. DB
43575.421	vis	59.0	–0.00281	BBSAG No. 37	45671.411	vis	1879.0	0.01309	BAV Lichten. DB
43788.475	vis	244.0	–0.00113	BBSAG No. 39	45672.550	vis	1880.0	0.00005	BAV Lichten. DB
43803.446	vis	257.0	–0.00137	BBSAG No. 39	45694.427	vis	1899.0	–0.00359	BBSAG No. 70
43865.645	vis	311.0	0.00939	Baldwin and Samolyk 1993	45701.340	vis	1905.0	–0.00040	BBSAG No. 70
43870.241	vis	315.0	–0.00115	BBSAG No. 41	45915.546	vis	2091.0	0.00166	BBSAG No. 73
43878.302	vis	322.0	–0.00159	BBSAG No. 41	45993.864	vis	2159.0	0.00853	Baldwin and Samolyk 1993
43932.426	vis	369.0	–0.00439	BBSAG No. 42	45998.461	vis	2163.0	–0.00100	BBSAG No. 74
44132.808	vis	543.0	–0.00673	Baldwin and Samolyk 1993	46000.769	vis	2165.0	0.00373	Baldwin and Samolyk 1993
44132.819	vis	543.0	0.00427	Baldwin and Samolyk 1993	46005.375	vis	2169.0	0.00319	BBSAG No. 74
44139.717	vis	549.0	–0.00753	Baldwin and Samolyk 1993	46006.520	vis	2170.0	–0.00344	BBSAG No. 74
44189.246	vis	592.0	0.00120	BBSAG No. 45	46007.674	vis	2171.0	–0.00107	Baldwin and Samolyk 1993
44192.692	vis	595.0	–0.00770	Baldwin and Samolyk 1993	46029.553	vis	2190.0	–0.00312	Baldwin and Samolyk 1993
44214.578	vis	614.0	–0.00275	Baldwin and Samolyk 1993	46050.284	vis	2208.0	–0.00154	BBSAG No. 75
44222.645	vis	621.0	0.00281	Baldwin and Samolyk 1993	46052.592	vis	2210.0	0.00319	Baldwin and Samolyk 1993
44266.401	vis	659.0	–0.00329	BBSAG No. 46	46060.653	vis	2217.0	0.00276	Baldwin and Samolyk 1993
44267.538*	vis	660.0	–0.01792	BAV Lichten. DB	46060.659	vis	2217.0	0.00876	BAV Lichten. DB
44311.316	vis	698.0	–0.00202	BBSAG No. 47	46119.392	vis	2268.0	0.00842	BBSAG No. 76
44449.509*	vis	818.0	–0.00511	BBSAG No. 49	46172.365	vis	2314.0	0.00625	BBSAG No. 76
44472.551	vis	838.0	0.00421	BBSAG No. 49	46318.623	vis	2441.0	0.00671	BBSAG No. 78
44474.844	vis	840.0	–0.00606	Baldwin and Samolyk 1993	46357.773	vis	2475.0	0.00115	Baldwin and Samolyk 1993
44539.342	vis	896.0	0.00043	BBSAG No. 51	46377.348	vis	2492.0	–0.00163	BBSAG No. 79
44549.703	vis	905.0	–0.00328	Baldwin and Samolyk 1993	46416.509	vis	2526.0	0.00381	BBSAG No. 79
44555.467	vis	910.0	0.00255	BBSAG No. 51	46439.542	vis	2546.0	0.00413	Baldwin and Samolyk 1993
44608.443	vis	956.0	0.00338	BBSAG No. 52	46447.606	vis	2553.0	0.00669	Baldwin and Samolyk 1993

table continued on following pages

Table 3. Available times of minima and O–C residuals from Equation 1, cont.

Epoch HJD 2400000+	*Type*	*Cycle*	*O–C*	*Reference*	*Epoch HJD 2400000+*	*Type*	*Cycle*	*O–C*	*Reference*
46478.698	vis	2580.0	0.00457	Baldwin and Samolyk 1993	49220.703	vis	4961.0	–0.03127	Baldwin and Samolyk 1997
46629.556	vis	2711.0	–0.00150	BBSAG No. 80	49243.737	vis	4981.0	–0.02995	Baldwin and Samolyk 1997
46659.502	vis	2737.0	0.00201	BBSAG No. 81	49250.647	vis	4987.0	–0.02976	Baldwin and Samolyk 1997
46681.380	vis	2756.0	–0.00103	BBSAG No. 81	49266.771	vis	5001.0	–0.02863	Baldwin and Samolyk 1997
46713.625	vis	2784.0	–0.00179	Baldwin and Samolyk 1993	49326.650	vis	5053.0	–0.03461	Baldwin and Samolyk 1997
46736.662	vis	2804.0	0.00253	Baldwin and Samolyk 1993	49327.802	vis	5054.0	–0.03424	Baldwin and Samolyk 1997
46742.422	vis	2809.0	0.00436	BBSAG No. 82	49331.271	vis	5057.0	–0.02014	BBSAG No. 105
46744.721	vis	2811.0	0.00009	Baldwin and Samolyk 1993	49333.560	vis	5059.0	–0.03441	Baldwin and Samolyk 1997
46764.301	vis	2828.0	0.00231	BBSAG No. 82	49384.237	vis	5103.0	–0.02931	BBSAG No. 106
46765.454	vis	2829.0	0.00367	BBSAG No. 82	49455.638	vis	5165.0	–0.02963	Baldwin and Samolyk 1997
46804.606	vis	2863.0	0.00011	Baldwin and Samolyk 1993	49561.586	vis	5257.0	–0.03197	BBSAG No. 107
46805.756	vis	2864.0	–0.00152	Baldwin and Samolyk 1993	49637.594	vis	5323.0	–0.03182	Baldwin and Samolyk 1997
46817.280	vis	2874.0	0.00614	BBSAG No. 83	49637.596	vis	5323.0	–0.02982	Baldwin and Samolyk 1997
46820.735	vis	2877.0	0.00624	Baldwin and Samolyk 1993	49650.258	vis	5334.0	–0.03580	BBSAG No. 108
47001.557*	vis	3034.0	0.02168	BAV Lichten. DB	49713.599	vis	5389.0	–0.03467	Baldwin and Samolyk 1997
47039.531	vis	3067.0	–0.00825	BBSAG No. 85	49713.602	vis	5389.0	–0.03167	Baldwin and Samolyk 1997
47063.711*	vis	3088.0	–0.01256	Baldwin and Samolyk 1993	49715.913	vis	5391.0	–0.02394	Saijo 1997
47069.481	vis	3093.0	–0.00073	BBSAG No. 87	49774.636	vis	5442.0	–0.03428	Baldwin and Samolyk 1997
47084.449	vis	3106.0	–0.00398	BBSAG No. 86	49787.307	vis	5453.0	–0.03126	BBSAG No. 108
47086.749	vis	3108.0	–0.00724	Baldwin and Samolyk 1993	49789.608	vis	5455.0	–0.03352	Baldwin and Samolyk 1997
47109.776	vis	3128.0	–0.01293	Baldwin and Samolyk 1993	49810.337	vis	5473.0	–0.03394	BBSAG No. 109
47185.790	vis	3194.0	–0.00678	Baldwin and Samolyk 1993	49810.339	vis	5473.0	–0.03194	BBSAG No. 109
47200.763	vis	3207.0	–0.00502	Baldwin and Samolyk 1993	49948.534	vis	5593.0	–0.03303	BBSAG No. 110
47205.374	vis	3211.0	–0.00056	BBSAG No. 87	49965.807	vis	5608.0	–0.03454	Baldwin and Samolyk 1997
47235.301	vis	3237.0	–0.01605	BBSAG No. 88	50041.817	vis	5674.0	–0.03240	Baldwin and Samolyk 1997
47390.769	vis	3372.0	–0.01865	Baldwin and Samolyk 1993	50047.570	vis	5679.0	–0.03757	Baldwin and Samolyk 1997
47411.513	vis	3390.0	–0.00407	BBSAG No. 89	50047.573	vis	5679.0	–0.03457	Baldwin and Samolyk 1997
47411.513	vis	3390.0	–0.00407	Baldwin and Samolyk 1993	50068.305	vis	5697.0	–0.03198	BBSAG No. 111
47420.714	vis	3398.0	–0.01614	Baldwin and Samolyk 1993	50099.402	vis	5724.0	–0.02910	BBSAG No. 111
47435.694	vis	3411.0	–0.00738	BAV Lichten. DB	50154.674	vis	5772.0	–0.03554	Baldwin and Samolyk 1997
47456.412	vis	3429.0	–0.01880	BBSAG No. 90	50167.335	vis	5783.0	–0.04252	BBSAG No. 111
47480.602	vis	3450.0	–0.01311	Baldwin and Samolyk 1993	50313.597	vis	5910.0	–0.03805	BBSAG No. 113
47524.367	vis	3488.0	–0.01021	BBSAG No. 90	50337.776	vis	5931.0	–0.04337	Baldwin and Samolyk 1997
47554.306	vis	3514.0	–0.01370	BBSAG No. 91	50380.389	vis	5968.0	–0.04083	BBSAG No. 113
47554.312	vis	3514.0	–0.00770	BBSAG No. 91	50397.671	vis	5983.0	–0.03334	Baldwin and Samolyk 1997
47556.608	vis	3516.0	–0.01497	Baldwin and Samolyk 1993	50420.693	vis	6003.0	–0.04402	Baldwin and Samolyk 1997
47562.368	vis	3521.0	–0.01314	BBSAG No. 91	50427.605	vis	6009.0	–0.04183	Baldwin and Samolyk 1997
47564.668	vis	3523.0	–0.01640	Baldwin and Samolyk 1993	50433.357	vis	6014.0	–0.04800	BBSAG No. 114
47822.640	vis	3747.0	–0.01045	Baldwin and Samolyk 1993	50486.342	vis	6060.0	–0.03817	BBSAG No. 114
47823.786	vis	3748.0	–0.01608	Baldwin and Samolyk 1993	50488.642	vis	6062.0	–0.04144	Baldwin and Samolyk 1997
47837.607	vis	3760.0	–0.01469	Baldwin and Samolyk 1993	50495.557	vis	6068.0	–0.03624	Baldwin and Samolyk 1997
47850.281	vis	3771.0	–0.00867	BBSAG No. 94	50509.371	vis	6080.0	–0.04185	BBSAG No. 114
47858.341	vis	3778.0	–0.01011	BBSAG No. 93	50509.378	vis	6080.0	–0.03485	BBSAG No. 114
47911.312	vis	3824.0	–0.01427	BBSAG No. 94	50516.282	vis	6086.0	–0.04065	BBSAG No. 114
47934.345	vis	3844.0	–0.01396	BBSAG No. 94	50517.430	vis	6087.0	–0.04429	BBSAG No. 114
47943.557	vis	3852.0	–0.01503	Baldwin and Samolyk 1993	50518.583	vis	6088.0	–0.04292	Baldwin and Samolyk 1997
48209.580	vis	4083.0	–0.01951	Baldwin and Samolyk 1993	50541.611	vis	6108.0	–0.04760	Baldwin and Samolyk 1997
48222.254	vis	4094.0	–0.01349	BBSAG No. 97	50692.476	vis	6239.0	–0.04667	BBSAG No. 115
48232.616	vis	4103.0	–0.01619	Baldwin and Samolyk 1993	50752.363	vis	6291.0	–0.04465	BBSAG No. 116
48260.254	vis	4127.0	–0.01741	BBSAG No. 97	50761.571	vis	6299.0	–0.04972	Baldwin and Samolyk 2002
48260.258	vis	4127.0	–0.01341	BBSAG No. 97	50762.724	vis	6300.0	–0.04836	Baldwin and Samolyk 2002
48329.354	vis	4187.0	–0.01546	BBSAG No. 97	50769.633	vis	6306.0	–0.04916	Baldwin and Samolyk 2002
48490.578	vis	4327.0	–0.02024	BBSAG No. 98	50774.244	vis	6310.0	–0.04470	BBSAG No. 116
48506.705	vis	4341.0	–0.01611	Baldwin and Samolyk 1993	50782.305	vis	6317.0	–0.04514	BBSAG No. 116
48512.461	vis	4346.0	–0.01829	BAV Lichten. DB	50845.644	vis	6372.0	–0.04601	Baldwin and Samolyk 2002
48512.461	vis	4346.0	–0.01789	Baldwin and Samolyk 1993	51057.544	vis	6556.0	–0.04669	BBSAG No. 118
48534.340	vis	4365.0	–0.02033	BBSAG No. 99	51133.547	vis	6622.0	–0.05154	Baldwin and Samolyk 2002
48536.641	vis	4367.0	–0.02260	Baldwin and Samolyk 1993	51156.585	vis	6642.0	–0.04623	Baldwin and Samolyk 2002
48564.280	vis	4391.0	–0.02282	BBSAG No. 99	51177.313	vis	6660.0	–0.04764	BBSAG No. 119
48625.322	vis	4444.0	–0.01743	BBSAG No. 100	51383.4540	CCD	6839.0	–0.04915	BAV Lichten. DB
48686.346	vis	4497.0	–0.03004	BBSAG No. 100	51438.731	vis	6887.0	–0.05058	Baldwin and Samolyk 2002
48686.362	vis	4497.0	–0.01404	BBSAG No. 101	51469.8278	PE	6914.0	–0.04791	Nelson 2000
48893.645	vis	4677.0	–0.02518	Baldwin and Samolyk 1997	51490.5576	CCD	6932.0	–0.04752	Baldwin and Samolyk 2002
48923.588	vis	4703.0	–0.02467	Baldwin and Samolyk 1997	51513.589	vis	6952.0	–0.04880	Baldwin and Samolyk 2002
49005.351	vis	4774.0	–0.02769	BBSAG No. 103	51544.687	vis	6979.0	–0.04492	Baldwin and Samolyk 2002
49066.395	vis	4827.0	–0.02060	BAV Lichten. DB	51551.598	vis	6985.0	–0.04373	Baldwin and Samolyk 2002
49066.402	vis	4827.0	–0.01360	BAV Lichten. DB	51557.356	vis	6990.0	–0.04390	BBSAG No. 122

table continued on next page

Table 3. Available times of minima and O–C residuals from Equation 1, cont.

Epoch HJD 2400000+	Type	Cycle	O–C	Reference	Epoch HJD 2400000+	Type	Cycle	O–C	Reference
51580.391	vis	7010.0	–0.04158	BBSAG No. 122	54116.2733	CCD	9212.0	–0.05761	Doğru *et al.* 2009
51581.542	vis	7011.0	–0.04222	Baldwin and Samolyk 2002	54172.7032	CCD	9261.0	–0.05779	BAV Lichten. DB
51582.691	vis	7012.0	–0.04485	Baldwin and Samolyk 2002	54476.7360	CCD	9525.0	–0.05639	Samolyk 2008
51625.296	vis	7049.0	–0.05031	BBSAG No. 122	54521.6495	CCD	9564.0	–0.05662	Samolyk 2008
51809.563	vis	7209.0	–0.04477	BBSAG No. 123	54830.2903	CCD	9832.0	–0.05377	Hübscher *et al.* 2009
51870.594	vis	7262.0	–0.05038	Baldwin and Samolyk 2002	54830.2909	CCD	9832.0	–0.05317	Hübscher *et al.* 2009
51878.658	vis	7269.0	–0.04782	Baldwin and Samolyk 2002	54848.7164	CCD	9848.0	–0.05381	Diethelm 2009
51893.6265	CCD	7282.0	–0.05056	Baldwin and Samolyk 2002	54863.6886	CCD	9861.0	–0.05286	Samolyk 2009
51913.219*	vis	7299.0	–0.03584	BBSAG No. 124	54863.6887	CCD	9861.0	–0.05276	Samolyk 2009
51946.6017	CCD	7328.0	–0.05053	Baldwin and Samolyk 2002	54868.2952	CCD	9865.0	–0.05279	Doğru *et al.* 2009
51952.3600*	PE	7333.0	–0.05040	BBSAG No. 124	55105.5329	CCD	10071.0	–0.05172	Erkan *et al.* 2010
51961.5738	CCD	7341.0	–0.04967	Baldwin and Samolyk 2002	55122.8078	CCD	10086.0	–0.05133	Samolyk 2010
52205.724	vis	7553.0	–0.04591	Baldwin and Samolyk 2002	55127.4097	CCD	10090.0	–0.05597	Erkan *et al.* 2010
52212.634	vis	7559.0	–0.04571	BBSAG No. 126	55130.8691	CCD	10093.0	–0.05147	Samolyk 2010
52227.601	vis	7572.0	–0.04996	Baldwin and Samolyk 2002	55205.7253	CCD	10158.0	–0.05149	Diethelm 2010
52250.636	vis	7592.0	–0.04764	Baldwin and Samolyk 2002	55500.5411	CCD	10414.0	–0.05403	Doğru *et al.* 2011
52265.589*	vis	7605.0	–0.06588	BAV Lichten. DB	55501.6927	CCD	10415.0	–0.05406	Samolyk 2011
52279.423	vis	7617.0	–0.05149	BBSAG No. 127	55502.8443	CCD	10416.0	–0.05409	Diethelm 2011
52530.479*	vis	7835.0	–0.05173	Diethelm 2003	55571.9411	CCD	10476.0	–0.05534	Nagai 2012
52555.8134	PE	7857.0	–0.05328	Nelson 2003	55579.4331*	CCD	10482.5	–0.04896	Hübscher 2011
52585.751	vis	7883.0	–0.05817	BAV Lichten. DB	55837.9646	CCD	10707.0	–0.05932	Samolyk 2012
52637.572	vis	7928.0	–0.06070	BAV Lichten. DB	55867.9069	CCD	10733.0	–0.05951	Diethelm 2012
52637.575	vis	7928.0	–0.05770	BAV Lichten. DB	55970.4010	CCD	10822.0	–0.06085	Hoňková *et al.* 2013
52652.550	vis	7941.0	–0.05415	BAV Lichten. DB	55970.4011	CCD	10822.0	–0.06075	Hoňková *et al.* 2013
52658.3078	PE	7946.0	–0.05432	Diethelm 2003	55970.4011	CCD	10822.0	–0.06075	Hoňková *et al.* 2013
52902.454	vis	8158.0	–0.05455	Diethelm 2004	56015.3147	CCD	10861.0	–0.06088	Hoňková *et al.* 2013
52966.940	vis	8214.0	–0.06006	BAV Lichten. DB	56015.3151	CCD	10861.0	–0.06053	Hoňková *et al.* 2013
53290.5507	CCD	8495.0	–0.05855	Zejda *et al.* 2006	56186.9049	CCD	11010.0	–0.06416	Samolyk 2013a
53326.2516	CCD	8526.0	–0.05831	Nagai 2004a	56230.6663	CCD	11048.0	–0.06486	Samolyk 2013a
53342.375	vis	8540.0	–0.05778	Locher 2005	56238.7280	CCD	11055.0	–0.06460	Samolyk 2013a
53351.5880	CCD	8548.0	–0.05786	BAV Lichten. DB	56262.9112	CCD	11076.0	–0.06571	Nagai 2013
53359.6483	CCD	8555.0	–0.05900	BAV Lichten. DB	56262.9126	CCD	11076.0	–0.06431	Samolyk 2015
53410.3205	PE	8599.0	–0.05870	Hübscher *et al.* 2005	56520.8743	CCD	11300.0	–0.06866	Samolyk 2013b.
53594.576*	vis	8759.0	–0.06466	Locher 2005	56654.4619	CCD	11416.0	–0.07061	Hoňková *et al.* 2015
53654.4681	CCD	8811.0	–0.05753	Hübscher *et al.* 2006	56654.4622	CCD	11416.0	–0.07031	Hoňková 2*et al.* 015
53733.938*	vis	8880.0	–0.05039	Nagai 2004b	56692.4656	CCD	11449.0	–0.07084	Hoňková *et al.* 2015
53755.8120	CCD	8899.0	–0.05743	BAV Lichten. DB	56692.4659	CCD	11449.0	–0.07054	Hoňková *et al.* 2015
53761.5703*	CCD	8904.0	–0.05730	BAV Lichten. DB	56953.8846	CCD	11676.0	–0.07279	Samolyk 2015
54044.8725	CCD	9150.0	–0.05710	BAV Lichten. DB	57355.8055	CCD	12025.0	–0.07219	Samolyk 2016
54059.8435	CCD	9163.0	–0.05734	BAV Lichten. DB					

**These minima timings deviated significantly for the O–C trend and were not used in the period analysis.*

Table 4. Orbital period jumps of XZ Per.

Cycle Interval	ΔT (days)	ΔP (10^{-5} days)	ΔP (seconds)
–16000 to –9900	–0.1163 ± 0.0106	–0.80 ± 0.07	–0.69 ± 0.06
–9900 to –7200	–0.0422 ± 0.0152	0.64 ± 0.18	0.56 ± 0.15
–7200 to –6400	0.0641 ± 0.0087	–0.72 ± 0.13	–0.62 ± 0.11
–6400 to 2600	–0.0063 ± 0.0003	0.38 ± 0.01	0.33 ± 0.01
2600 to 6700	0.0332 ± 0.0018	–0.70 ± 0.04	–0.60 ± 0.03
6700 to 8600	–0.0087 ± 0.0050	–0.02 ± 0.07	–0.02 ± 0.06
8600 to 10100	–0.1055 ± 0.0044	1.10 ± 0.05	0.95 ± 0.04
10100 to 11500	0.0704 ± 0.0080	–0.62 ± 0.08	–0.54 ± 0.07
11500 to 12400	–0.0632 ± 0.0044	0.54 ± 0.04	0.46 ± 0.03

2 and 3 of Table 5. No appreciable third light contribution was seen in the lights. The values for the g' and B passbands were very small, while the longer wavelengths, r', i', and V, were both small and negative. The normalized light curves for each passband, overlaid by the synthetic solution curves, are shown in Figure 8 with the residuals in Figure 9.

3.4. Spot model

The asymmetries in the light curves seen in Figures 8 and 9 are usually attributed to cool spots, hot regions such as faculae, or gas streams that impact one of the stars. At orbital phase 0.9 there is an excess of light seen in all the light curves. The residuals in Figure 9 show a sharp cutoff in this excess light when the stars approach primary eclipse. This feature is most likely caused by a hot spot on the primary star. Mass transferred from the Roche lobe filling secondary star would impact the primary star on its trailing side close to the equator (Zhang *et al.* 2014). An additional feature seen in the light curve residuals of Figure 9 is a light loss centered between orbital phase 0.3 to 0.4 for the DS1 observations. This indicates an under luminous region (cool spot) on the larger secondary star at the time the DS1 observations were acquired. This feature is not apparent in the DS2 data that were obtained six months later. Using BM3, a hot and cool spot were modeled for the DS1 observations and a single hot spot for DS2. The spot parameter's latitude,

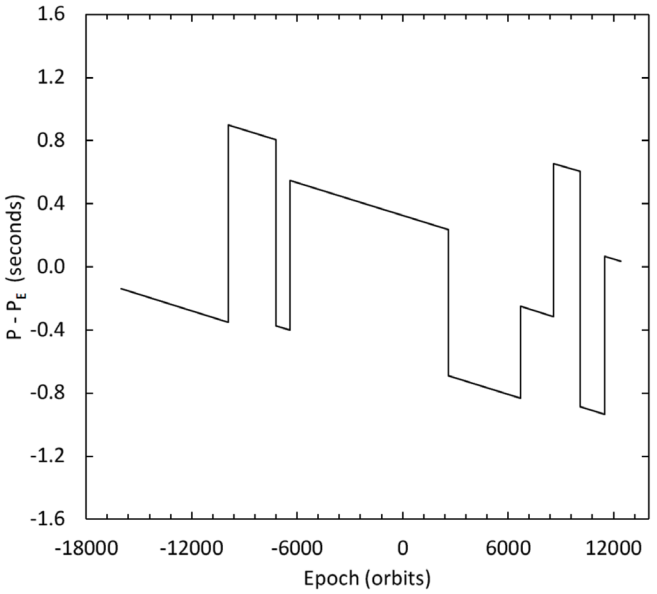

Figure 5. Orbital period changes of XZ Per as a function of time.

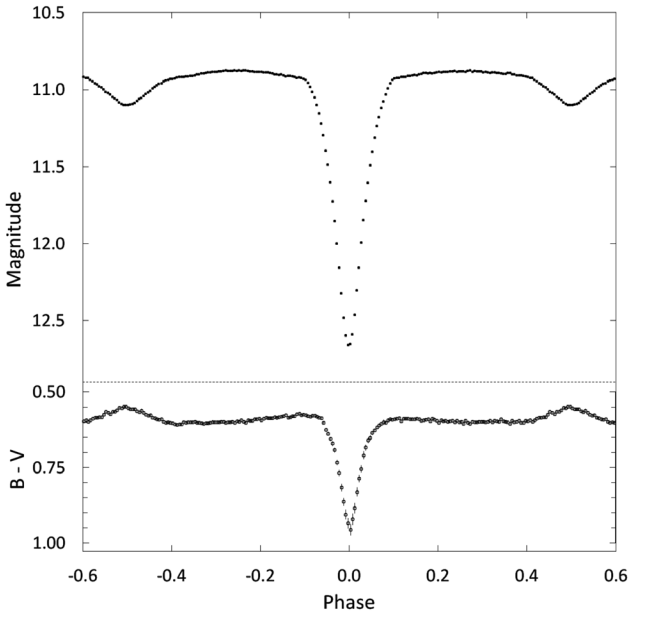

Figure 6. Light curve of all V-band observations in standard magnitudes (top panel). The observations were binned with a phase width of 0.005. The errors for each binned point are about the size of the plotted points. The B–V colors were calculated by subtracting the binned V magnitudes from the linearly interpolated binned B magnitudes.

longitude, size, and temperature were adjusted until a good fit resulted between the synthetic and observed light curves. New WD solutions were then made using the spot parameters from the BM3 fits. The best-fit WD spotted solution parameters are shown in columns 4 and 5 in Table 5. Figure 10 shows the final spotted model fits (solid lines) to the observed light curves and Figure 11 the residuals. For the DS1 solutions the sum of the residuals squared was 0.52 for the spotted model and 0.77 for the unspotted model (1.5 times larger) and for the DS2 solutions 0.26 for the spotted model and 0.54 for the unspotted model (2.1 times larger). A graphical representation of the spotted DS1 model is shown in Figure 12.

4. Discussion

The WD solutions indicate XZ Per is an evolved semi-detached system with the less massive secondary star filling its Roche lobe. Figure 13 compares the mass and radius of both stars with 61 semi-detached systems with well determined absolute parameters (Ibanoğlu *et al.* 2006). The primary star of XZ Per is close to the ZAMS like most of the other primaries in this group. The secondary along with all the other secondary stars in the sample are located on or above the TAMS line. The absolute stellar parameters of XZ Per can now be estimated. A main-sequence star with an effective temperature of 6680 K gives a mass of 1.41 ± 0.08 $M_\odot$ (Pecaut and Mamajeck 2013). Using the mass ratio from the WD solution gives the secondary star's mass as 0.92 ± 0.06 $M_\odot$ and applying Kepler's Third Law gives a distance between the mass centers of 6.125 ± 0.005 $R_\odot$. The mean stellar densities, $\bar{\rho}_1 = 0.39 \pm 0.01$ g cm^{-3} and $\bar{\rho}_2 = 0.14 \pm 0.03$ g cm^{-3}, were found using Mochnacki's (1981) empirical relationship

$$\bar{\rho}_1 = \frac{0.0189}{r_1^3(1+q)\,P^2} \text{ and } \bar{\rho}_2 = \frac{0.0189q}{r_2^3\,(1+q)\,P^{2'}}, \qquad (6)$$

where the stellar radius is normalized to the semi-major axis and P is in days. The visual luminosities, $L_{1V} = 5.87 \pm 0.56\ L_\odot$ and $L_{2V} = 1.20 \pm 0.30\ L_\odot$, were calculated using the bolometric magnitudes from the WD light curve program (LC) and bolometric corrections (Pecaut and Mamajek 2013). The LC output also provided the stellar radii and surface gravities of each star. All the estimated stellar parameters have been collected in Table 6. The distance to this system was determined from the precision parallax measurements of the Gaia spacecraft (Gaia 2016). The measured parallax is p = 0.00234 ± 0.00023, which gives a distance of d = 427 ± 48 pc. Assuming no interstellar extinction, this distance combined with the apparent V magnitude at orbital phase 0.25 gives an absolute magnitude of $M_V = 2.73 \pm 0.05$. This value compares well with the absolute magnitudes from the DS1 and DS2 model solutions, $M_V = 2.74 \pm 0.10$ and $M_V = 2.77 \pm 0.10$, respectively. If the spectroscopically determined effective temperature for the primary star is accurate, these values indicate the interstellar extinction is likely small (a few hundredths of a magnitude). A higher temperature primary, on the other hand, would point to a larger extinction value. A precision spectroscopic study would be necessary to confirm the temperature of the primary star as well as provide direct determination of the stellar masses.

Mass transfer can occur in semi-detached systems when the secondary star fills its Roche lobe. The main-sequence primary is on the receiving end of the matter stream. Given the short orbital period of XZ Per, the distance between the two stars is small compared to their radii. The mass stream would likely be narrow and would directly impact the primary star near its equator, creating a small hot spot due to impact heating (Zhang *et al.* 2014; Ibanoğlu *et al.* 2006). The locations and sizes of the hot spots modeled in both WD solutions are consistent with an active mass stream from the secondary to the primary star. Additional small distortions in the light

Table 5. XZ Per synthetic light curve solutions.

parameter	*DS1–g′, r′, i′ no spots*	*DS2–B,V no spots*	*DS1–g′, r′, i′ with spots*	*DS2–B,V with spots*
i (°)	85.05 ± 0.42	84.97 ± 0.08	85.15 ± 0.11	85.03 ± 0.05
T_1 (K)	[1]6680	[1]6680	[1]6680	[1]6680
T_2 (K)	4624 ± 7	4636 ± 8	4628 ± 11	4636 ± 5
$q(M_2/M_1)$	0.638 ± 0.013	0.629 ± 0.004	0.647 ± 0.005	0.637 ± 0.003
Ω_1	4.195 ± 0.038	4.272 ± 0.017	4.195 ± 0.013	4.247 ± 0.012
Ω_2	3.131	3.116	3.149	3.131
$L_1/(L_1+L_2)$ (B)	—	0.8906 ± 0.0002	—	0.8949 ± 0.0002
$L_1/(L_1+L_2)$ (V)	—	0.8185 ± 0.0005	—	0.8244 ± 0.0003
$L_1/(L_1+L_2)$ (g')	0.8650 ± 0.0023	—	0.8644 ± 0.0004	—
$L_1/(L_1+L_2)$ (r')	0.7802 ± 0.0035	—	0.7788 ± 0.0007	—
$L_1/(L_1+L_2)$ (i')	0.7337 ± 0.0041	—	0.7318 ± 0.0008	—
r_1 pole	0.2703 ± 0.0020	0.2724 ± 0.0013	0.2818 ± 0.0011	0.2779 ± 0.0010
r_1 point	0.2813 ± 0.0022	0.2848 ± 0.0016	0.2964 ± 0.0014	0.2918 ± 0.0012
r_1 side	0.2747 ± 0.0021	0.2771 ± 0.0014	0.2872 ± 0.0012	0.2831 ± 0.0011
r_1 back	0.2790 ± 0.0022	0.2821 ± 0.0015	0.2930 ± 0.0013	0.2887 ± 0.0012
r_2 pole	0.3095 ± 0.0019	0.3179 ± 0.0006	0.3185 ± 0.0006	0.3198 ± 0.0004
r_2 point	0.4417 ± 0.0019	0.4524 ± 0.0006	0.4530 ± 0.0006	0.4547 ± 0.0004
r_2 side	0.3234 ± 0.0020	0.3324 ± 0.0006	0.3330 ± 0.0007	0.3344 ± 0.0004
r_2 back	0.3557 ± 0.0020	0.3646 ± 0.0006	0.3651 ± 0.0006	0.3665 ± 0.0004
$\sum res^2$	0.77	0.52	0.54	0.26
spot parameters			*Star 1-Hot Spot*	*Star 1-Hot Spot*
colatitude (°)	—	—	90 ± 14	72 ± 2
longitude (°)	—	—	21 ± 3	10 ± 1
spot radius (°)	—	—	10 ± 3	10 ± 2
temp.-factor	—	—	1.13 ± 0.07	1.17 ± 0.04
			Star 2-Cool Spot 1	
colatitude (°)	—	—	46 ± 18	—
longitude (°)	—	—	73 ± 4	—
spot radius (°)	—	—	24 ± 8	—
temp.-factor	—	—	0.85 ± 0.09	—

[1] *Assumed.*

Note: The errors in the stellar parameters result from the least–squares fit to the model. The actual uncertainties of the parameters are considerably larger (ex. T_1 and T_2 have uncertainties of about ± 180 K).

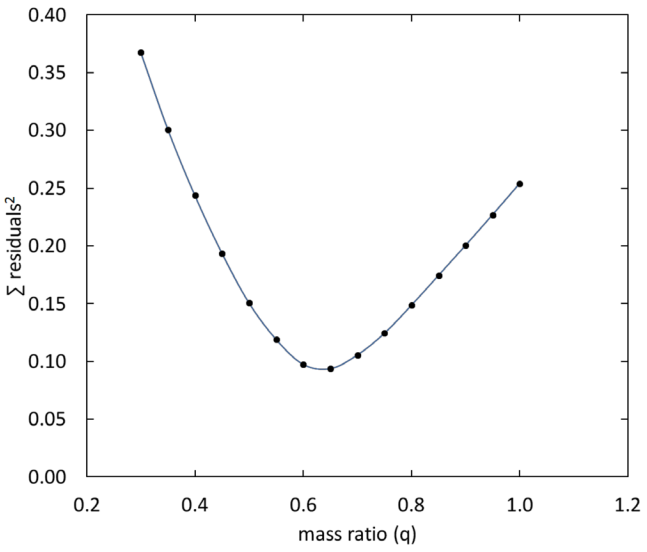

Figure 7. Results of the q-search showing the relation between the sum of the residuals squared and the mass ratio q.

curves at other orbital phases may also be effects of the impact heating, as diffusion and convection transport energy beyond the impact region.

The conservative mass transfer supported by the impact heating on the primary star would result in the widening of the orbit and an increasing period (Huang 1963). The least-squares solution for the quadratic ephemeris (section 3) gives a secular period decrease of $dP/dt = -1.27 \times 10^{-7}$ d yr^{-1}. This observed period decrease indicates the mass and angular momentum for the two stars is not conserved. Magnetic braking, which requires a stellar wind and a stellar magnetic field, is a possible cause of the angular momentum loss. XZ Per has a late-type secondary (spectral type K4) with a deep convective envelope. This convection combined with its rapid rotation should make the star magnetically active. The dark spot modeled on the secondary star and the changes in spot configuration between the two observational data sets is a good indication of magnetic activity. This could be the mechanism causing the mass and angular momentum loss and the resulting decrease in the orbital period (Hall 1989). There are a number of other Algols that have decreasing orbital periods with comparable dP/dt values (21 in Table 6 of Yang and Wei 2009). In addition, a

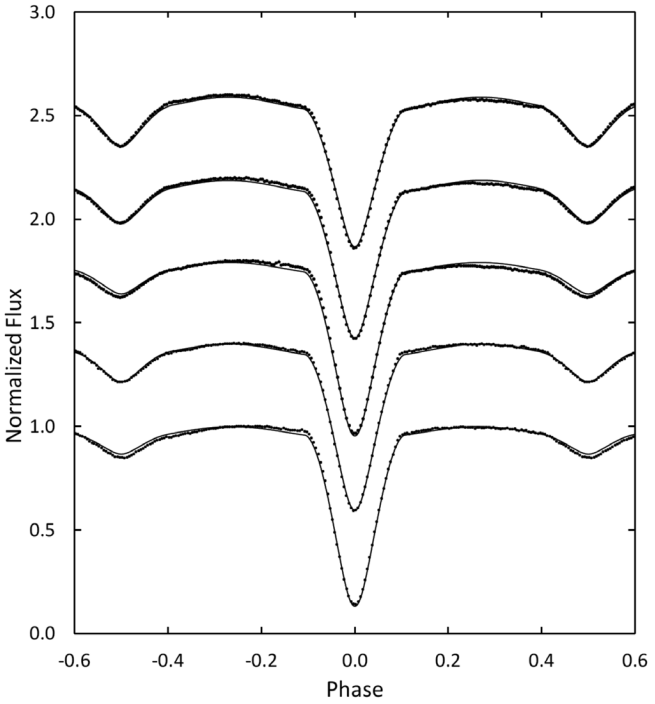

Figure 8. The WD model fit without spots (solid curve) to the observed normalized flux curves for each passband. From top to bottom the passbands are Sloan i', Sloan r', Sloan g', Johnson V, and Johnson B. Each curve is offset by 0.2 for this combined plot. The best-fit parameters are given in columns 2 and 3 of Table 5. Error bars are omitted from the points for clarity.

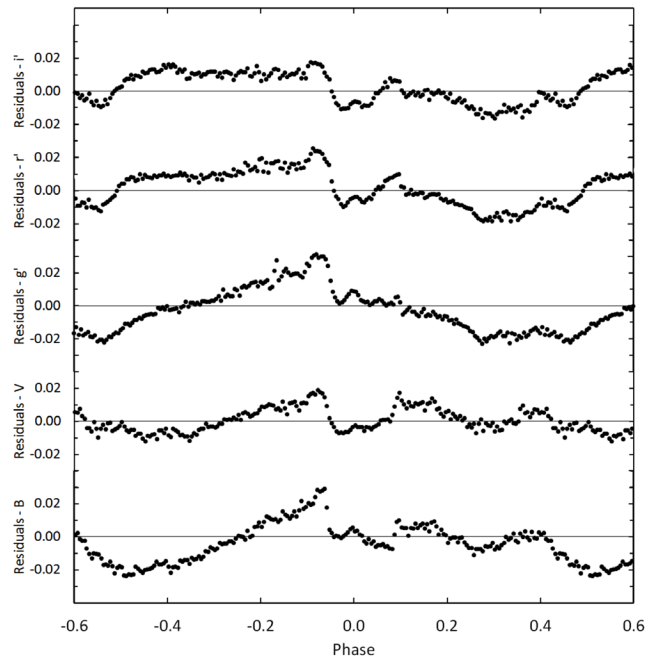

Figure 9. The residuals for the best-fit WD model without spots. Error bars are omitted from the points for clarity.

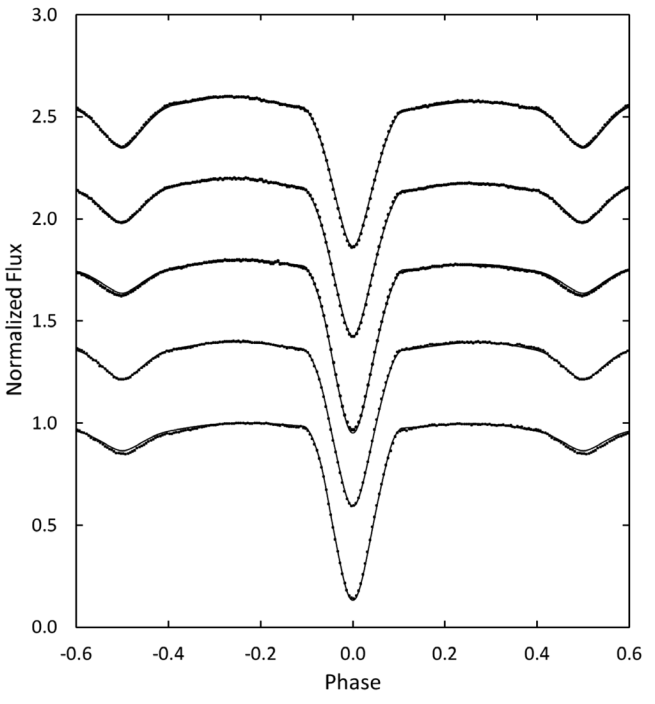

Figure 10. The WD model fit with spots (solid curve) to the observed normalized flux curves for each passband. From top to bottom the passbands are Sloan i', Sloan r', Sloan g', Johnson V, and Johnson B. Each curve is offset by 0.2 for this combined plot. The best-fit parameters are given in columns 4 and 5 of Table 5. Error bars are omitted from the points for clarity.

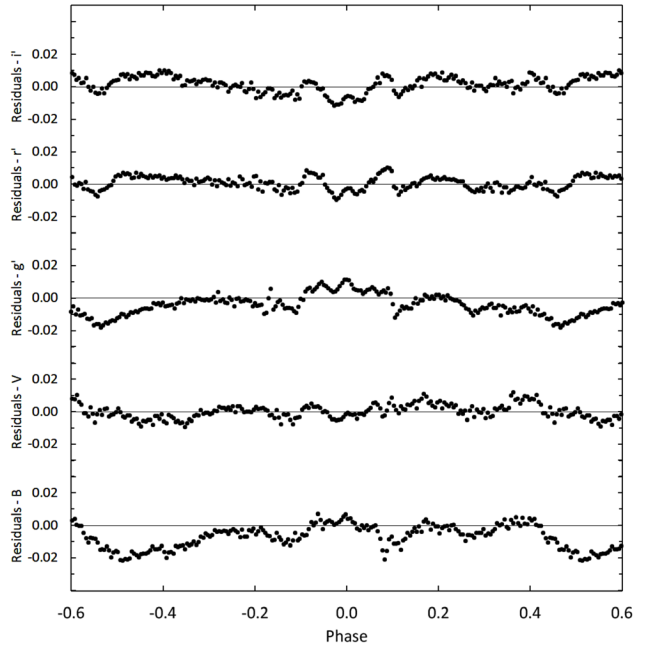

Figure 11. The residuals for the best-fit WD models with spots. Error bars are omitted from the points for clarity.

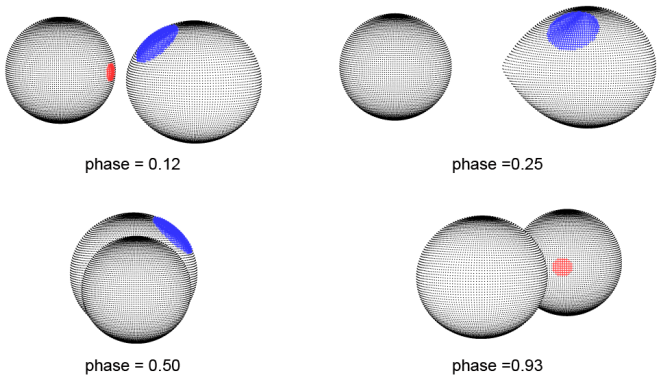

Figure 12. Roche Lobe surfaces of the best-fit WD spot DS1 model with orbital phase shown below each diagram.

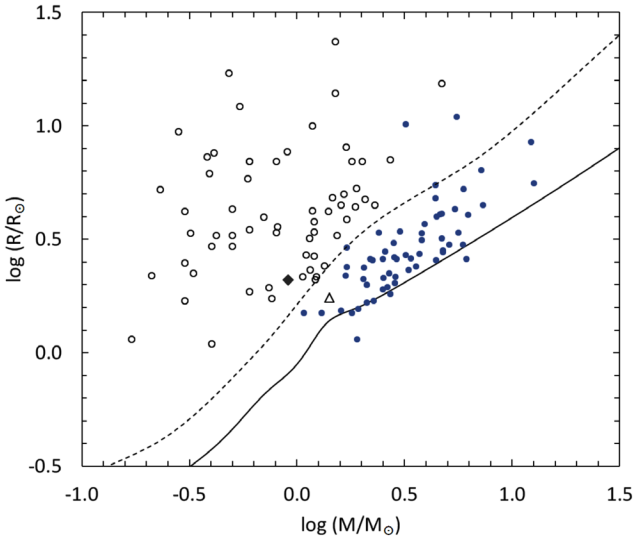

Figure 13. Positions of both components of XZ Per on the Mass–Radius diagram of 62 semi-detached Algol systems with well determined parameters. Closed circles are the primary stars and open circles the secondary stars. The triangle and the diamond are the primary and the secondary of XZ Per, respectively. Solid and dotted lines refer to ZAMS and TAMS, respectively, calculated from Tout *et al.* (1996).

number of Algol systems (RW CrB, TU Her, BO Mon, Y Psc, AY Gem, UU And, TY Peg, X Tri, and Z Per) also show sudden period jumps superimposed on secular decreasing periods that are similar to XZ Per (Qian 2000a, 2000b, 2001a, 2001b, 2002). The possible mechanism for the observed alternating period changes in semi-detached binaries was discussed by van 'T Veer (1993) and investigated by Qian (2002), who finds both the secular period decrease and the irregular period jumps can be explained by the variable interplay between magnetic coupling and spin orbit coupling. A secular period decrease could also result from a small fraction of the transferred mass forming a circumbinary disk (Chen *et al.* 2006). Detailed calculations indicate the orbital angular momentum can be efficiently removed by a thin disk surrounding both stars, but observations of XZ Per with time-resolved spectroscopy found no evidence of emission from a gaseous disk (Kaitchuck and Honeycutt 1982).

The observed light curves and photometric solutions of XZ Per look very similar to EP Cas, AK CMi, FG Gem, and DF Pup, which were classified as near contact binaries (NCB) (Yang *et al.* 2013) where the secondary star fills the Roche lobe and the primary is inside one. Yakut and Eggleton (2005)

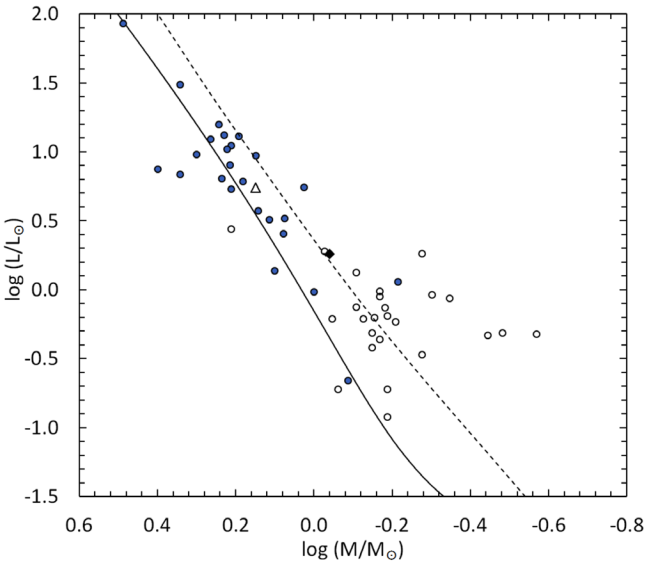

Figure 14. Positions of both components of XZ Per on the Mass–Luminosity diagram of 25 semi-detached NCB Algol systems with well determined parameters. Closed circles are the primary stars and open circles the secondary stars. The triangle and diamond are the primary and the secondary of XZ Per, respectively. Solid and dotted lines refer to ZAMS and TAMS, respectively, calculated from Tout *et al.* (1996).

Table 6. Provisional stellar parameters for XZ Per.

Parameter	*Symbol*	*Value*
Stellar masses	$M_1 (M_\odot)$	1.41 ± 0.08
	$M_2 (M_\odot)$	0.91 ± 0.06
Semi-major axis	$a (R_\odot)$	6.120 ± 0.005
Stellar radii	$R_1 (R_\odot)$	1.75 ± 0.03
	$R_2 (R_\odot)$	2.09 ± 0.12
Surface gravity	log g_1 (cgs)	4.10 ± 0.03
	log g_2 (cgs)	3.76 ± 0.04
Mean density	$\bar{\rho}_1$ (g cm^{-3})	0.37 ± 0.01
	$\bar{\rho}_2$ (g cm^{-3})	0.14 ± 0.03
Stellar luminosity	$L_{1V} (L_\odot)$	5.9 ± 0.6
	$L_{2V} (L_\odot)$	1.2 ± 0.3
Bolometric magnitude	$M_{bol,1}$	2.9 ± 0.1
	$M_{bol,2}$	4.1 ± 0.2

Values in this table are provisional. Radial velocity observations are necessary for direct determination of M_1, M_2, and a.

compiled a list of 25 NCBs with well determined parameters. Figure 14 shows a mass luminosity diagram (M-L) of the components of these binaries with XZ Per included. The primary star of XZ Per (open triangle in Figure 14) lies about midway between the zero-age main-sequence (ZAMS) line and the terminal-age main-sequence (TAMS), as do most of the other NCB primary stars. XZ Per's secondary star (filled diamond in Figure 14) lies close to the TAMS, again indicating it has evolved. Most of the other secondary stars in this NCB sample are at a similar point in their evolution. The filling factor for the primary star can determine how close the star is to filling its lobe. It is defined as $f_1 = R_1 / R_L$, where R_1 is the radius

of the primary star and R_L is the volume radius of the Roche lobe. Eggleton's (1983) formula gives R_L/a as a function of mass ratio (q),

$$\frac{R_L}{a} = \frac{0.49q^{2/3}}{0.6q^{2/3} + \ln(1 + q^{1/3})'}, \quad (7)$$

where a is the separation between the star's mass centers. Using the photometric solution from DS1 gives a value of $f_1 = 84\%$, which is higher than many semi-detached binaries that show a secular period decrease (Yang and Wei 2009). XZ Per appears to be at an intermediate evolutionary state, beginning life as a close detached binary and eventually, with additional mass and angular momentum loss, becoming a W UMa contact binary (Yakut and Eggleton 2005). Model calculations indicate XZ Per should start its contact phase 4–5 Gyr after its formation with the two stars ultimately coalescing into a single star (Gazeas and Stepień 2008).

5. Conclusions

Two new sets of photometric observations of XZ Per resulted in five complete light curves that were used for investigation of this system. Based on these observations, photometric solutions were obtained for both data sets. The results of a detailed analysis of the DS1 observations and the period study gave the following results:

1. XZ Per is a semi-detached Algol-type eclipsing binary with a mass ratio of q = 0.647 and an orbital inclination of i = 85.2°. The effective temperature of the primary star is $T_1 = 6680$ K, and the secondary $T_2 = 4628$ K. The primary is a F3 main-sequence star and the secondary an evolved K4 star (possibly a subgiant). No third light was found in the system but a hot spot was modeled on the primary star and a large cool spot on the secondary. Mass transferred from the secondary star is the likely cause of the hot spot on the primary. The cool spot was not necessary for the DS2 solution, indicating a changing spot configuration and therefore a magnetically active secondary star.

2. The period study found a secular decrease in the orbital period at a rate of $dP/dt = -1.27 \times 10^{-7}$ d yr^{-1}. Magnetic braking is likely the mechanism causing mass and angular momentum loss. In addition, the *(O–C)* data displayed several alternating period jumps superimposed on the secular decrease. The fill-out of 84% for the primary star indicates a near contact configuration. With additional angular momentum and mass loss, the fill-out of the primary star will continue to increase as the orbital period decreases until it eventually fills its Roche lobe.

Future spectroscopic and precision photometric observations would be important in monitoring orbital period changes and would allow determination of absolute parameters.

6. Acknowledgements

This research was made possible through the use of the AAVSO Photometric All-Sky Survey (APASS), funded by the Robert Martin Ayers Sciences Fund. This research has made use of the VizieR catalogue access tool and data from the SIMBAD database (operated at CDS, Strasbourg, France), the European Space Agency (ESA) mission Gaia (http://www.cosmos.esa.int/gaia), and the Lichtenknecker-Database of the BAV. The author would especially like to acknowledge the observers of AAVSO, BAV, VSOLJ, and other organizations that provided observations spanning several decades. Without their tireless efforts, the period study in this paper would not have been possible. The author is grateful to Norman Markworth for his careful reading of the manuscript and his valuable comments and suggestions.

References

Baldwin, M. 1974, *J. Amer. Assoc. Var. Star Obs.*, **3**, 60.
Baldwin, M. 1975, *J. Amer. Assoc. Var. Star Obs.*, **4**, 86.
Baldwin, M. 1976a, *J. Amer. Assoc. Var. Star Obs.*, **5**, 29**.**
Baldwin, M. 1976b, *J. Amer. Assoc. Var. Star Obs.*, **5**, 84.
Baldwin, M. 1977, *J. Amer. Assoc. Var. Star Obs.*, **6**, 24.
Baldwin, M. E., and Samolyk, G. 1993, *Observed Minima Timings of Eclipsing Binaries, Number 1*, (https://www.aavso.org/observed-minima-timings-eclipsing-binaries)
Baldwin, M. E., and Samolyk, G. 1997, *Observed Minima Timings of Eclipsing Binaries, Number 4*, (https://www.aavso.org/observed-minima-timings-eclipsing-binaries)
Baldwin, M. E., and Samolyk, G. 2002, *Observed Minima Timings of Eclipsing Binaries, Number 7*, (https://www.aavso.org/observed-minima-timings-eclipsing-binaries)
Beob. der Schweizerischen Astron. Ges. (BBSAG). 1972–2002, *BBSAG Bull.,* Nos. 2–127 (https://www.calsky.com/cs.cgi/Deep-Sky/8/3?&lang=en).
Berliner Arb. Veränderl. Sterne. 2015, Lichtenknecker-Database of the BAV (http://www.bav-astro.eu/index.php/veroeffentlichungen/lichtenknecker-database)
Bradstreet, D. H., and Steelman, D. P. 2002, *Bull. Amer. Astron. Soc.*, **34**, 1224.
Brancewicz, H. K., and Dworak, T. Z. 1980, *Acta Astron.*, **30**, 501.
Budding, E., Erdem, A., Çiçek, C., Bulut, I., Soydugan, F., Soydugan, E., Bakiş, V., and Demircan, O. 2004, *Astron. Astrophys.*, **417**, 263.
Chen, W.-C., Li, Z.-D., and Qian, S.-B. 2006, *Astrophys. J.*, **649**, 973.
Diethelm, R. 2003, *Inf. Bull. Var. Stars*, No. 5438, 1.
Diethelm, R. 2004, *Inf. Bull. Var. Stars*, No. 5543, 1.
Diethelm, R. 2009, *Inf. Bull. Var. Stars*, No. 5894, 1.
Diethelm, R. 2010, *Inf. Bull. Var. Stars*, No. 5945, 1.
Diethelm, R. 2011, *Inf. Bull. Var. Stars*, No. 5960, 1.
Diethelm, R. 2012, *Inf. Bull. Var. Stars*, No. 6011, 1.
Doğru, S. S., Erdem, A., Aliçavuş, F., Akin, T., and Kanvermez, C. 2011, *Inf. Bull. Var. Stars*, No. 5988, 1.
Doğru, S. S., Erdem, A., Donmez, A., Bulut, A., Akin, T., Dogru, D., Çiçek, C., and Soydugan, F. 2009, *Inf. Bull. Var. Stars*, No. 5893, 1.
Eggleton, P. P. 1983, *Astrophys. J.*, **268**, 368.
Erkan, N., Erdem, A., Akin, T., Aliçavuş, F., and Soydugan, F. 2010, *Inf. Bull. Var. Stars*, No. 5924, 1.

Flin, P. 1969, *Inf. Bull. Var. Stars*, No. 328, 1.
Gaia Collaboration, *et al.* 2016, *Astron. Astrophys.*, **595A**, 2 (Gaia Data Release 1).
Gazeas, K., and Stepień, K. 2008, *Mon. Not. Roy. Astron. Soc.*, **390**, 1577.
Hall, D. S. 1989, *Space Sci. Rev.*, **50**, 219.
Henden, A. A., *et al.* 2014, AAVSO Photometric All-Sky Survey, data release 9, (https://www.aavso.org/apass).
Hoňková, K. *et al.* 2013, *Open Eur. J. Var. Stars*, No. 160, 1.
Hoňková, K. *et al.* 2015, *Open Eur. J. Var. Stars*, No. 168, 1.
Huang, S. S. 1963, *Astrophys. J.*, **138**, 471
Hübscher, J. 2011, *Inf. Bull. Var. Stars*, No. 5984, 1.
Hübscher, J., Paschke, A., and Walter, F. 2005, *Inf. Bull. Var. Stars*, No. 5657, 1.
Hübscher, J., Paschke, A., and Walter, F. 2006, Inf. Bull. Var. Stars, No. 5731, 1.
Hübscher, J., Steinbach, H.-M., and Walter, F. 2009, *Inf. Bull. Var. Stars*, No. 5889, 1.
Ibanoğlu, C. *et al.* 2006, *Mon. Not. Roy. Astron. Soc.*, **373**, 435.
Kafka, S. 2015, variable star observations from the AAVSO International Database (https://www.aavso.org/aavso-international-database).
Kaitchuck, R. H., and Honeycutt, R. K. 1982, *Publ. Astron. Soc. Pacific*, **94**, 532.
Kaitchuck, R. H., Honeycutt, R. K., and Schlegel, E. M. 1985, *Publ. Astron. Soc. Pacific*, **97**, 1178.
Klimek, Z. 1972, *Inf. Bull. Var. Stars*, No. 637, 1.
Klimek, Z. 1973, *Inf. Bull. Var. Stars*, No. 779, 1.
Kreiner, J. M. 1971, *Acta Astron.*, **21**, 365.
Kurucz, R. L. 1993, in *Light Curve Modeling of Eclipsing Binary Stars*, ed. E. F. Milone, IAU Symp. 151, Springer, New York, 93.
Lavrov, M. I. 1971, *Soviet Astron.*, **15**, 2, 236.
Locher, K. 2005, *Open Eur. J. Var. Stars*, No. 3, 1.
Lucy, L. B. 1968, *Astrophys. J.*, **151**, 1123.
Malkov, O. Yu., Oblak, E., Snegireva, E. A., and Torra, J. 2006, *Astron. Astrophys.*, **446**, 785.
Mallama, A. D. 1980, *Astrophys. J., Suppl. Ser.*, **44**, 241.
Mirametrics. 2015, Image Processing, Visualization, Data Analysis, (http://www.mirametrics.com)
Mochnacki, S. W. 1981, *Astrophys. J.*, **245**, 650.
Nagai, K. 2004a, *Bull. Var. Star Obs. League Japan*, No. 43, 5.
Nagai, K. 2004b, *Bull. Var. Star Obs. League Japan*, No. 44, 7.
Nagai, K. 2012, *Bull. Var. Star Obs. League Japan*, No. 53, 6.
Nagai, K. 2013, *Bull. Var. Star Obs. League Japan*, No. 55, 6.
Nelson, R. 2000, *Inf. Bull. Var. Stars*, No. 4840, 1.
Nelson, R. 2003, *Inf. Bull. Var. Stars*, No. 5371, 1.
Pecaut, M. J., and Mamajek, E. E. 2013, *Astrophys. J., Suppl. Ser.*, **208**, 9 (http://www.pas.rochester.edu/~emamajek/EEM_dwarf_UBVIJHK_colors_Teff.txt).
Popper, D. M. 1996, *Astrophys. J., Suppl. Ser.*, **106**, 133.
Qian, S. 2000a, *Astron. J.*, 119, 901.
Qian, S. 2000b, *Astron. J.*, 119, 3064.
Qian, S. 2001a, *Astron. J.*, 121, 1614.
Qian, S. 2001b, *Astron. J.*, 122, 1561.
Qian, S. 2002, *Publ. Astron. Soc. Pacific*, **114**, 650.
Robinson, I. J. 1967, *Inf. Bull. Var. Stars*, No. 221, 3.
Ruciński, S. M. 1969, *Acta Astron.*, **19**, 245.
Saijo, K. 1997, *Bull. Var. Star Obs. League Japan*, No. 23, 1.
Samolyk, G. 2008, *J. Amer. Assoc. Var. Star Obs.*, **36**, 171.
Samolyk, G. 2009, *J. Amer. Assoc. Var. Star Obs.*, **37**, 44.
Samolyk, G. 2010, *J. Amer. Assoc. Var. Star Obs.*, **38**, 183.
Samolyk, G. 2011, *J. Amer. Assoc. Var. Star Obs.*, **39**, 177.
Samolyk, G. 2012, *J. Amer. Assoc. Var. Star Obs.*, **40**, 975.
Samolyk, G. 2013, *J. Amer. Assoc. Var. Star Obs.*, **41**, 122.
Samolyk, G. 2013, *J. Amer. Assoc. Var. Star Obs.*, **41**, 328.
Samolyk, G. 2015, *J. Amer. Assoc. Var. Star Obs.*, **43**, 77.
Samolyk, G. 2016, *J. Amer. Assoc. Var. Star Obs.*, **44**, 69.
Samus, N. N., Kazarovets, E. V., Durlevich, O. V., Kireeva, N. N., and Pastukhova, E. N. 2017, *Astron. Rep.*, **61**, 80 (*General Catalogue of Variable Stars*, version GCVS 5.1.; http://www.sai.msu.su/gcvs/gcvs/index.htm).
Szafraniec, R. 1960, *Acta Astron.*, **10**, 99.
Terrell, D., and Wilson, R. E. 2005, *Astrophys. Space Sci.*, **296**, 221.
Todoran, I. 1967, *Inf. Bull. Var. Stars*, No. 187, 1.
Tout, C. A., Pols, O. R., Eggleton, P. P., and Han, Z. 1996, *Mon. Not. Roy. Astron. Soc.*, **281**, 257.
van Hamme, W. 1993, *Astron. J.*, **106**, 2096.
van Hamme, W., and Wilson, R. E. 1998, *Bull. Amer. Astron. Soc.*, 30, 1402.
Van 'T Veer, F. 1993, in *New Frontiers in Binary Star Research*, ed. K.-C. Leung, I.-S. Nha, ASP Conf. Ser. 38, 229.
Whitney, B. S. 1959, *Astron. J.*, **64**, 258**.**
Wilson, R. E. 1978, *Astrophys. J.*, **224**, 885.
Wilson, R. E., and Devinney, E. J. 1971, *Astrophys. J.*, **166**, 605.
Wood, B. D., and Forbes, J. E. 1963, *Astron. J.*, **68**, 257.
Yakut, K., and Eggleton, P. P. 2005, *Astrophys. J.*, **629**, 1055.
Yang, Y.-G., Dai, H.-F., He, J.-J., Zhang, J., and Ding, W. 2013, *Publ. Astron. Soc. Japan*, **65**, 45.
Yang, Y.-G., and Wei, J.-Y. 2009, *Astron. J.*, **137**, 226.
Zejda, M., Mikulasek, Z., and Wolf, M. 2006, *Inf. Bull. Var. Star*s, No. 5741, 1.
Zhang, J., Qian, S.-B., and Jiang, L.-Q. 2014, *Res. Astron. Astrophys.*, **14**, 179.